

## RESEARCH ARTICLE

10.1002/2016JD024890

## Key Points:

- Magnetic field changes from 1900 to 2000 cause significant changes in temperature and wind in the whole atmosphere system (0–500 km) in DJF.
- Direct responses form in the thermosphere and propagate downward dynamically, initially via the gravity wave-induced residual circulation.
- In the middle atmosphere, changes in planetary waves become also important, but these may not be correctly represented in the SH.

## Correspondence to:

I. Cnossen,  
inos@bas.ac.uk;  
icnossen@yahoo.com

## Citation:

Cnossen, I., H. Liu, and H. Lu (2016), The whole atmosphere response to changes in the Earth's magnetic field from 1900 to 2000: An example of "top-down" vertical coupling, *J. Geophys. Res. Atmos.*, *121*, 7781–7800, doi:10.1002/2016JD024890.

Received 2 FEB 2016

Accepted 22 JUN 2016

Accepted article online 27 JUN 2016

Published online 9 JUL 2016

## The whole atmosphere response to changes in the Earth's magnetic field from 1900 to 2000: An example of "top-down" vertical coupling

Ingrid Cnossen<sup>1</sup>, Hanli Liu<sup>2</sup>, and Hua Lu<sup>1</sup>

<sup>1</sup>British Antarctic Survey, Cambridge, UK, <sup>2</sup>National Center for Atmospheric Research, Boulder, Colorado, USA

**Abstract** We study the effects of changes in the Earth's magnetic field between 1900 and 2000 on the whole atmosphere (0–500 km altitude), based on simulations with the Whole Atmosphere Community Climate Model eXtension. Magnetic field changes directly affect the temperature and wind in the upper atmosphere ( $> \sim 110$  km) via Joule heating and the ion drag force. However, we also find significant responses in zonal mean temperature and zonal wind in the Southern Hemisphere (SH) middle- to high-latitude troposphere, stratosphere, and mesosphere of up to  $\pm 2$  K and  $\pm 2$  m/s, as well as regionally significant changes in Northern Hemisphere (NH) polar surface temperatures of up to  $\pm 1.3$  K, in December–January–February. In the SH, changes in gravity wave filtering in the thermosphere induce a change in the residual circulation that extends down into the upper mesosphere, where further changes in the mean wind climatology are generated, together with changes in local planetary wave generation and/or amplification and gravity wave filtering. This induces further changes to a residual circulation cell extending down into the troposphere. However, inaccuracies in the simulated SH upper mesospheric wind climatology probably mean that the simulated temperature and wind responses in the SH lower and middle atmosphere are also inaccurate. The NH middle atmosphere response is zonally asymmetric, consisting of a significant change in the positioning and shape of the upper stratospheric polar vortex, which is dynamically consistent with the surface temperature response. However, the downward coupling mechanism in the NH is generally less clear.

### 1. Introduction

The Earth's internal magnetic field, generated in the liquid outer core, gradually changes over time. Even on a multidecadal to centennial timescale, considerable changes can occur. During the past century, the Earth's magnetic dip poles, where the magnetic field is exactly vertical, have typically been moving at a speed of  $\sim 10$  km/yr [Olsen and Manda, 2007]. The northern magnetic pole motion has even been speeding up since the 1970s to a speed of 40–60 km/yr [Newitt et al., 2002; Olsen and Manda, 2007]. At the same time, the magnetic dipole moment has been decreasing by about 5–7% per century since 1840 [Gubbins et al., 2006; Manda and Purucker, 2005]. The strongest changes in the Earth's magnetic field over the past few centuries have taken place over South America and the southern Atlantic Ocean, approximately corresponding to the South Atlantic Anomaly region. This is a low-intensity region of the Earth's magnetic field, which has deepened, increased in spatial extent, and drifted westward and slightly northward over time [e.g., Badhwar, 1997; Finlay et al., 2010].

The Earth's magnetic field affects the upper atmosphere in various ways: It influences the conductivity in the ionosphere and ionospheric plasma transport processes, controls the geographic locations of the magnetic equator and auroral zones, and guides the coupling of the ionosphere-thermosphere system with the solar wind and magnetosphere. Rishbeth [1984] and Takeda [1996] first discussed the implications of changes in the strength and configuration of the Earth's magnetic field for the ionosphere. The mechanisms by which changes in field strength and orientation affect the full ionosphere-thermosphere-magnetosphere system were examined in detail in a series of idealized modeling studies by Cnossen et al. [2011, 2012a, 2012b] and Cnossen and Richmond [2012]. In addition, Yue et al. [2008], Cnossen and Richmond [2008, 2013], and Cnossen [2014] showed how the actual changes in the Earth's magnetic field over the past century have affected the ionosphere and thermosphere. While magnetic field changes affect the ionosphere most directly, neutral temperature and wind patterns are significantly modified through collisions between charged and neutral particles, which result in Joule heating and the so-called "ion drag" force on the neutral winds.

It is not obvious that the magnetic field should have a significant influence on the atmosphere below the ionosphere and thermosphere. Especially an effect on tropospheric climate may seem far-fetched. Still, from time to time reports emerge that suggest a link between the Earth's magnetic field and surface climate. *Wollin et al.* [1971a, 1971b] may have been the first to propose such a link, based on deep-sea sediment cores from near the Cape Verde Islands, the Caribbean, the North Pacific, and the eastern Mediterranean. They found anticorrelations between the intensity and inclination of the Earth's magnetic field and climate indicators, such as oxygen isotope anomalies and the abundance of a specific group of planktonic foraminifera that is sensitive to temperature, over the past 470,000 to 1.2 Myr. Their results tentatively suggested that a stronger magnetic field and a larger inclination angle are associated with a colder climate. Anticorrelations between magnetic field intensity and surface temperature seem to occur on shorter timescales as well. *Gallet et al.* [2005] found that maxima and minima in the intensity of the Earth's magnetic field over western Europe from the seventeenth to nineteenth century coincide with cooling and warming events in that region, respectively, as evidenced by Alpine glacier advances and retreats. Similar evidence was reported by *King* [1975] and more recently by *De Santis et al.* [2012], who found a significant correlation between the size of the South Atlantic Anomaly region and global sea level since 1600. *Bakmutov* [2006] found that temperatures in Northeastern Europe were  $\sim 1\text{--}2$  K higher as the geomagnetic pole was receding from the region and  $\sim 1\text{--}2$  K lower when it was approaching the region, possibly indicating a similar anticorrelation between (local) magnetic field strength and surface temperature. In contrast, *Kitaba et al.* [2013] found evidence to suggest that a decrease in magnetic field strength is associated with tropospheric cooling.

Although these strands of evidence are intriguing, they remain very controversial, while there is no clear mechanism to explain the relationship between magnetic field variations and climate variability. Often the cosmic ray-cloud hypothesis is invoked to explain the relationship [e.g., *Courtylot et al.*, 2007; *Vieira et al.*, 2008; *Knudsen and Riisager*, 2009; *Kitaba et al.*, 2013]. The idea is that a stronger magnetic field results in greater shielding from cosmic rays and therefore a lower cosmic ray flux. As cosmic rays are thought to act as cloud condensation nuclei, fewer cosmic rays may be expected to lead to fewer clouds, which in turn would produce a change in the climate (e.g., temperature and rainfall). However, convincing proof of a causal link between cosmic rays and clouds remains elusive [e.g., *Laken et al.*, 2012]. It is also not possible yet to test the mechanism with global atmospheric models, because a detailed understanding of the microphysics involved is still lacking and not implemented in climate models. However, there are also other ways in which the Earth's magnetic field could potentially affect climate. A key possibility is that the magnetic field influences the lower atmosphere via its effects on the upper atmosphere. These effects could be communicated downward through dynamical, chemical, or electrical coupling processes. We will first consider dynamical coupling mechanisms, which will also be the focus of this study.

*Hines* [1974] first suggested that perturbations in the upper atmosphere might affect the atmosphere below by changing the conditions for planetary wave reflection or absorption. Changes in the zonal mean wind structure at higher levels in the atmosphere could lead to more/less wave reflection or absorption, or changes in the height of reflection, thereby altering the amplitudes and/or phases of planetary waves at lower altitudes. This mechanism has been shown to play a role in troposphere-stratosphere coupling [e.g., *Perlwitz and Harnik*, 2003, 2004]. However, since planetary waves generated in the troposphere do not tend to propagate upward as high as the thermosphere, it may not be possible to directly link the thermosphere and troposphere in this way. On the other hand, there is evidence for planetary wave generation in the upper mesosphere and lower thermosphere regions [*Holton*, 1984; *Smith*, 2003; *Mayr et al.*, 2004; *Funke et al.*, 2010], so that it could potentially offer a mechanism to link changes in the lower thermosphere down to the mesosphere. In addition, Hines' mechanism can in principle be applied to gravity waves as well, which can travel all the way from the troposphere up into the thermosphere [e.g., *Fritts and Alexander*, 2003; *Vadas and Liu*, 2009].

A second dynamical pathway of downward coupling is via the wave-driven residual circulation, corresponding to the equator-to-pole Brewer-Dobson circulation in the stratosphere, with an upward branch near the equator and downward branches near the poles, and a summer-to-winter circulation in the mesosphere, with an upward branch near the summer pole and a downward branch near the winter pole. *Haynes et al.* [1991] described in detail how a zonal mean wave force on the mean flow affects the residual circulation in the atmosphere below, a concept known as the "downward control" principle. A change in wave breaking at high altitude can therefore modify the strength or structure of the residual circulation, leading to changes in tracer transport and adiabatic heating/cooling via downwelling/upwelling.

Modeling studies by *Arnold and Robinson* [1998, 2001, 2003] showed that idealized forcings in the lower thermosphere affect the atmosphere below down to the lower stratosphere. They argued that this is due to the redirection of wave activity, as a result of changes in the background wind conditions in the lower thermosphere. However, the precise mechanism by which the perturbation is communicated downward, and the relative importance of planetary waves and gravity waves were not clear. Further, their model did not include a troposphere, so that any impact on tropospheric climate variability could not be assessed. On the other hand, it is likely that a perturbation that reaches the lower stratosphere will also affect the troposphere, as numerous studies have demonstrated that the lower stratosphere and troposphere are closely coupled [e.g., *Baldwin and Dunkerton*, 2001; *Christiansen*, 2001; *Thompson et al.*, 2002, 2005].

Chemical processes can also contribute to a downward communication of upper atmospheric changes. Energetic particle precipitation from the magnetosphere produces odd nitrogen (NO and NO<sub>2</sub>, also referred to as NO<sub>x</sub>) in the high-latitude mesosphere and thermosphere [e.g., *Solomon et al.*, 1982]. During polar winter, NO<sub>x</sub> can be sufficiently long-lived to be transported down to the stratosphere within the polar vortex, where it catalytically destroys stratospheric ozone. This leads to changes in stratospheric heating, and therefore changes in temperature and atmospheric dynamics, which can eventually influence the polar climate near the surface [e.g., *Baumgaertner et al.*, 2011]. Various studies have shown the importance of this mechanism of downward influence in the context of variations in geomagnetic activity [e.g., *Seppälä et al.*, 2007, 2013; *Randall et al.*, 2007; *Lu et al.*, 2008]. Since energetic particle precipitation is guided by the Earth's magnetic field, changes in the positioning of the geomagnetic poles could potentially modify this downward coupling mechanism.

A third type of vertical atmospheric coupling is via the global electric circuit [see, e.g., *Tinsley*, 2008]. The solar wind and interplanetary magnetic field (IMF) have a direct influence on the high-latitude electric field in the ionosphere, and changes in this electric field could conceivably affect the global electric circuit as a whole. This is thought to influence cloud microphysics in the troposphere, and thereby surface climate [*Tinsley*, 2008]. *Lam et al.* [2013, 2014] recently argued that this could explain observed meteorological responses to variations in the interplanetary magnetic field (IMF) carried by the solar wind. If this is correct, changes in the Earth's magnetic field will also be able to affect surface climate via this pathway as these have a significant effect on the ionospheric electric field as well [e.g., *Crossen et al.*, 2011, 2012a].

Recent developments in whole atmosphere modeling now make it possible to examine some of the pathways of vertical coupling from the thermosphere down to the troposphere. Here we use the Whole Atmosphere Community Climate Model eXtension (WACCM-X) to study how changes in the Earth's magnetic field between 1900 and 2000 have affected the atmosphere from the surface up to ~500 km altitude. WACCM-X incorporates the aforementioned dynamical and chemical pathways of vertical coupling but does not yet include the cosmic ray-cloud pathway nor a representation of the global electric circuit, although work is ongoing to include the latter [*Baumgaertner et al.*, 2013]. We are therefore only able to study the dynamical and NO<sub>x</sub>-ozone pathways here.

This paper is organized as follows. Section 2 provides further information on WACCM-X, the experimental setup, and the methods used to analyze the model outputs. Section 3 presents the effects of changes in the Earth's magnetic field between 1900 and 2000 on the whole atmosphere system, which includes significant changes in temperature and wind in the lower and middle atmosphere. In section 4 we analyze how these lower and middle atmosphere responses are formed. We find that the NO<sub>x</sub>-ozone mechanism plays an insignificant role in our results and therefore focus on dynamical coupling mechanisms. We finish with a discussion and conclusions in section 5.

## 2. Methods

We use simulations with the Whole Atmosphere Community Climate Model eXtension (WACCM-X) [*Garcia et al.*, 2007; *Liu et al.*, 2010], which is part of the Community Earth System Model (CESM), developed by the National Center for Atmospheric Research (NCAR). Here we used CESM release version 1.2.0. WACCM-X is a chemistry-climate model that extends globally from the surface to the thermosphere (up to ~500 km). It is based on NCAR's Community Atmosphere Model and includes all of the physical parameterizations of that model. In addition, WACCM-X incorporates a detailed neutral chemistry model for the middle atmosphere,

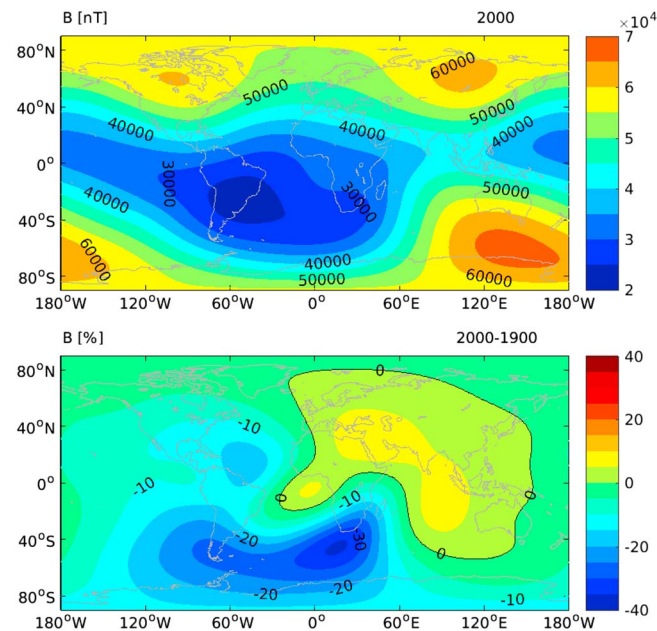


**Figure 1.** (top) Main magnetic field intensity in 2000 and (bottom) the percentage difference with 1900 according to the IGRF.

a model of ion chemistry in the mesosphere/lower thermosphere region, ion drag and auroral processes, parameterizations of extreme ultraviolet heating and infrared transfer under non-local thermodynamic equilibrium, and modified parameterizations of gravity wave effects and vertical diffusion. Effects of both orographic and nonorographic gravity waves are accounted for, with the latter including waves generated by deep convection and frontal systems [Richter et al., 2010]. The high-latitude electric potential pattern associated with magnetospheric convection is specified according to the Weimer [1996] model, and energetic particle precipitation from the magnetosphere is parameterized following Roble and Ridley [1987]. Since both processes are strongly organized by the Earth's magnetic field, they are specified in magnetic apex coordinates [Richmond, 1995].

The Earth's magnetic field in the model is specified by the International Geomagnetic Reference Field (IGRF) [Finlay et al., 2010], which is used both for the definition of the magnetic apex coordinate system and for any computations that involve the magnetic field.

Changes in the Earth's magnetic field affect processes that depend directly on the magnetic field (e.g.,  $\mathbf{E} \times \mathbf{B}$  plasma drifts, ion drag, and Joule heating), as well as the mapping of magnetic apex coordinates to geographic coordinates, resulting in changes in the geographic positioning and shape of the specified high-latitude electric potential and particle precipitation patterns. However, any changes in the magnitude of the electric potential or the energy or flux of energetic particles, which might arise from a change in the magnetic field, are not included in WACCM-X. Previous work with other models indicates that those effects are only significant for disturbed geomagnetic conditions [Cnossen and Richmond, 2013]. To avoid such effects, our simulations consider geomagnetically quiet conditions.

We compare two simulations set up with the magnetic field of the years 1900 and 2000, respectively, to characterize the climate during these two epochs. These simulations will be referred to as m1900 and m2000. In all other aspects the two simulations were set up identically, i.e., other long-term forcing factors (e.g., the rise in CO<sub>2</sub> concentration, changes in ozone concentration, and long-term variations in ocean circulation), are not considered here, and were kept fixed. The differences between our simulations therefore represent the atmospheric response to the change in magnetic field between 1900 and 2000. Figure 1 illustrates the changes in the magnetic field that occurred during this period. The main dipole moment decreased from  $\sim 8.3 \times 10^{22} \text{ Am}^2$  in 1900 to  $\sim 7.8 \times 10^{22} \text{ Am}^2$  in 2000, while the apex magnetic pole positions shifted by 223 km in the Southern Hemisphere (SH) and 305 km in the Northern Hemisphere (NH).

We ran the model with a horizontal resolution of  $1.9^\circ \times 2.5^\circ$  (latitude  $\times$  longitude) and 81 vertical levels. The vertical resolution varies from half a scale height in the mesosphere and thermosphere, to 1.75 km around the stratopause, and down to 1.1–1.4 km in the troposphere, except near the ground, where much higher vertical resolution is used. Both simulations used a fixed solar activity level ( $F_{10.7} = 200$  solar flux units) and fixed geomagnetic activity level ( $Kp = 2$ ) as input, representing quiet geomagnetic conditions. Under such conditions, the high-latitude forcings from the magnetosphere (electric potential and energetic particle precipitation) are relatively weak, so that the upper atmosphere response to the changes in the magnetic field simulated by the model represents a conservative estimate. We also note that WACCM generally underestimates NO<sub>x</sub> production by energetic particle precipitation compared to observations [e.g., Randall et al., 2015], so this is expected to be especially weak in our simulations. Randall et al. [2015] further found that downward transport

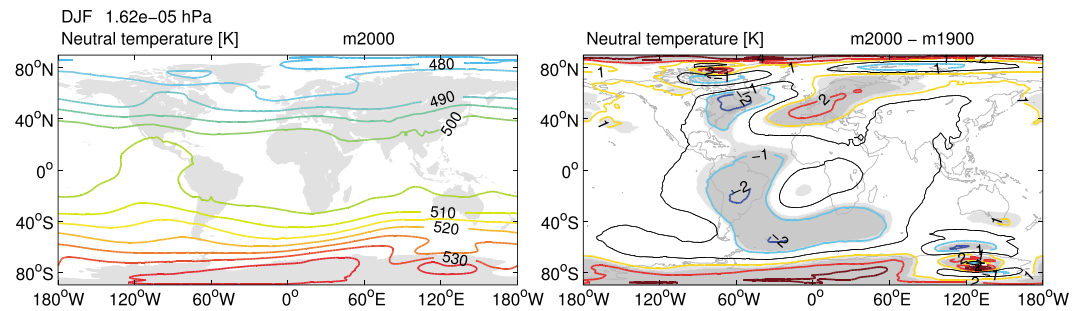


**Figure 2.** (left) Neutral temperature in the lower thermosphere ( $1.62 \times 10^{-5}$  hPa;  $\sim 130$  km) for m2000 and (right) the difference with m1900 (m2000-m1900) in DJF, with light and dark shading indicating statistical significance at the 95% and 99% levels, respectively.

of  $\text{NO}_x$  was also underestimated in their simulations. While they ran standard WACCM in specified dynamics mode rather than WACCM-X, WACCM-X is likely to suffer from similar problems, so that the  $\text{NO}_x$ -ozone mechanism is probably too weak in our simulations.

Each of our simulations was run for 38 years and 2 months. The first 2 months were discarded to allow for spin-up and to have 38 full years for the December-January-February (DJF) season. We analyze 38 year mean differences between the m2000 and m1900 simulations (m2000-m1900 hereafter) and use the 38 year standard deviations to calculate the statistical significance of these differences, according to a two-sided Student's  $t$  test. Each year is thus treated effectively as an independent ensemble member. To check the robustness of the results, we have also tested the effect of randomly excluding up to 8 years from the 38 year averages, still retaining at least 30 years' worth of data, which is the classic period over which the climate is normally defined. We find that excluding up to 8 years gives small changes in the significance of the differences between simulations, but the magnitudes and character of the differences remain very similar. We therefore stopped our simulations after 38 years and only show results from the analysis done with all 38 years.

### 3. Whole Atmosphere Response to Magnetic Field Changes

In the thermosphere, our WACCM-X simulations show a clear response to the changes in the Earth's magnetic field. The large-scale spatial structure and magnitude of these responses resemble those obtained by *Cnossen and Richmond* [2008, 2013] and *Cnossen* [2014] using upper atmosphere models for similar changes in the Earth's magnetic field (comparing similar pressure levels and seasons). We therefore consider the upper atmosphere effects produced by WACCM-X, which constitute the forcing that the rest of the atmosphere responds to, to be reasonable. Differences in temperature and winds between our simulations are significant for all seasons in the upper atmosphere (not shown). However, in the lower and middle atmosphere they are mainly found during DJF. Our analysis will therefore focus on this season hereafter.

Figure 2 shows the DJF mean temperature difference at a pressure level of  $1.6 \times 10^{-5}$  hPa ( $\sim 130$  km), as an example of the upper atmosphere forcing produced by the model. The largest differences in temperature occur near the locations of the (apex) magnetic poles. The Northern Hemisphere (NH) apex pole moved from (79.2°N/80.3°W) in 1900 to (81.9°N/83.3°W) in 2000, while the Southern Hemisphere (SH) apex pole moved from (76.2°S/126.8°E) in 1900 to (74.2°S/126.3°E) in 2000. These seemingly small shifts induce significant changes in the positioning and shape of the electric potential pattern at high latitudes and yield local differences on the order of 10–25% (not shown). This gives significant changes in ionospheric plasma velocities (i.e.,  $\mathbf{E} \times \mathbf{B}$  drifts), which affect the neutral atmosphere through ion drag (describing momentum exchange between charged and neutral particles taking place through collisions) and Joule heating (a frictional heating dependent on the difference between ion and neutral velocities). Neutral wind (not shown in Figure 2, but see Figure 3) and temperature patterns at high latitudes therefore also show primarily signs of a shift at high latitudes. In addition, there is an overall increase in temperature at high latitudes, which is due to an overall increase in Joule heating, associated with the weakening of the Earth's magnetic field, especially noticeable at southern high latitudes (a weaker magnetic field gives greater ionospheric conductivity and therefore

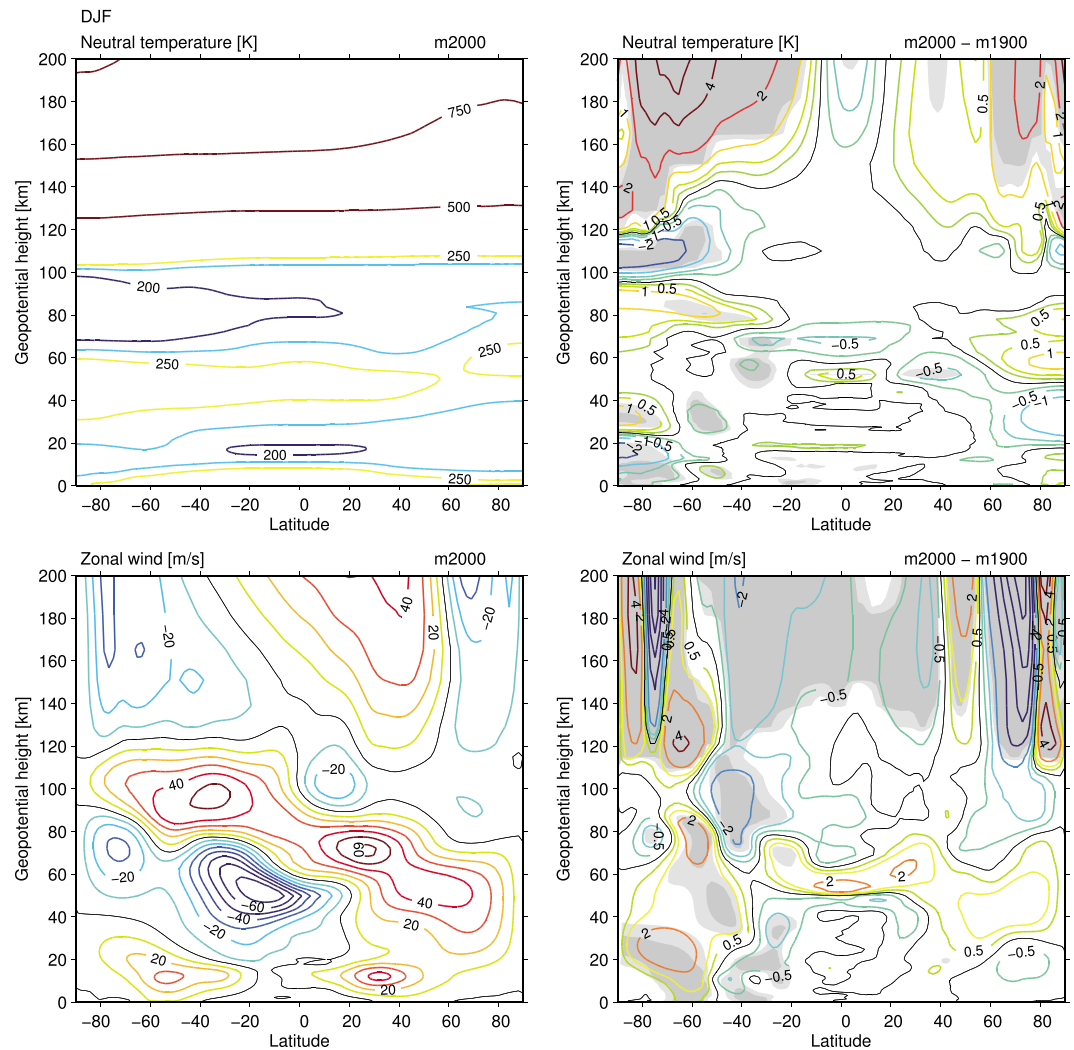


**Figure 3.** (top) Zonal mean neutral temperature and (bottom) zonal wind for (left) m2000 and (right) the difference with m1900 (m2000-m1900) in DJF, with light and dark shading indicating statistical significance at the 95% and 99% levels, respectively.

more Joule heating) [see *Crossen et al., 2012a*]. Differences in temperature and wind at lower latitudes are generally smaller, but they are strongest and most significant over South America and the southern Atlantic Ocean, corresponding to the area where the Earth’s magnetic field has changed the most over the past century [e.g., *Finlay et al., 2010*].

To describe the first-order response of the atmosphere as a whole, it is convenient to examine zonal mean differences first. Figure 3 shows zonal mean differences in the DJF mean temperature and zonal wind. The differences are clearly strongest in the thermosphere, as expected. The banded structure of the zonal wind responses in the high-latitude thermosphere is caused by shifts in the  $\mathbf{E} \times \mathbf{B}$  drift patterns, as explained above. Given that the NH middle atmosphere is generally more dynamically active than the SH, we had expected to see the largest differences in the middle atmosphere in the NH, especially during DJF (NH winter), when wave-mean flow interactions are strongest. However, the largest differences in the lower and middle atmosphere are in fact found in the SH, which are significant primarily at middle to high latitudes.

Around  $\sim 60^\circ\text{S}$ , the zonal wind in almost the entire column of air from the troposphere up to the lower thermosphere has become relatively more eastward. In the upper mesosphere the positive change in zonal wind at  $\sim 60^\circ\text{S}$  is flanked by two regions of negative change. This pattern suggests an upward and poleward shift of the climatological zonal wind structure, together with a vertical expansion (both downward and upward) of

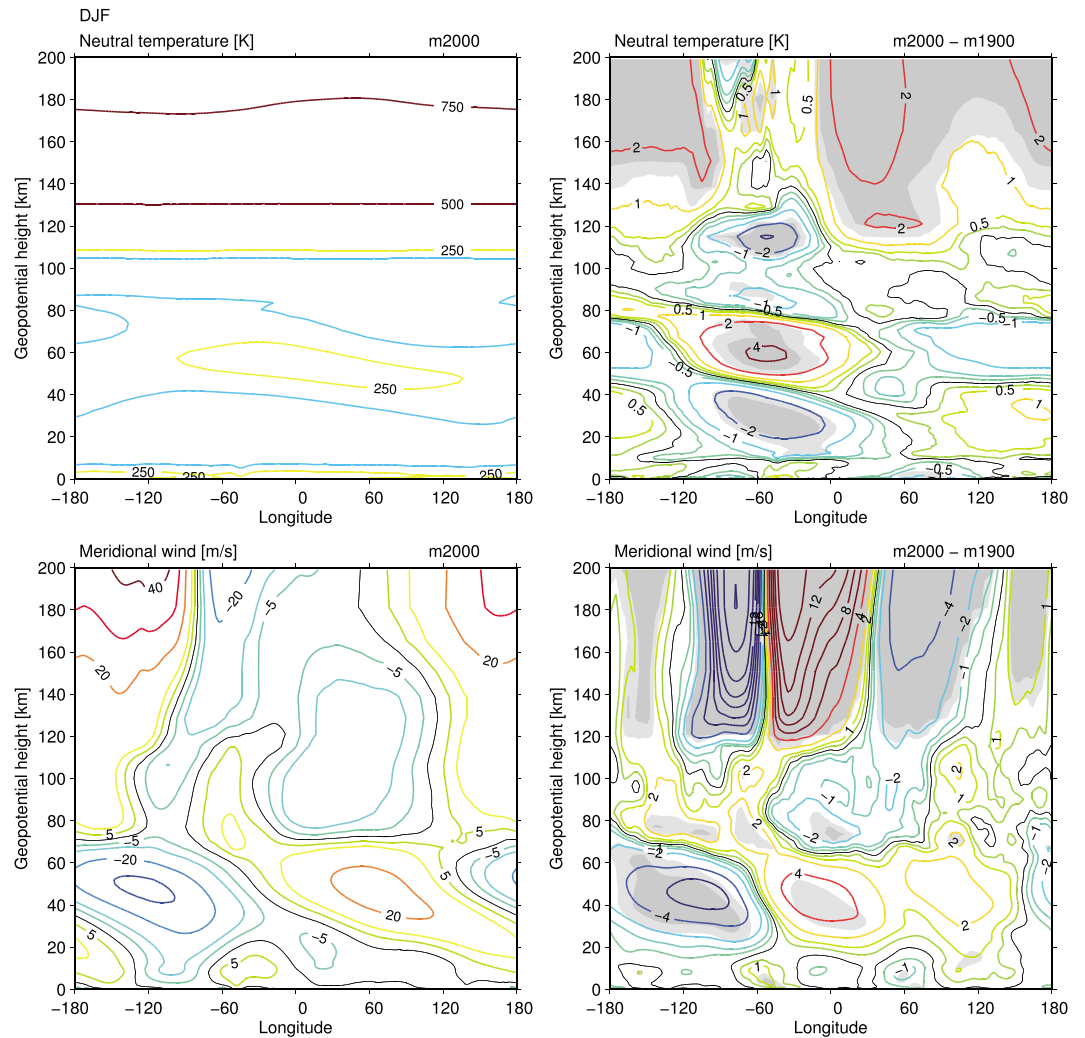


**Figure 4.** (top) Neutral temperature and (bottom) meridional wind at 65°N for (left) m2000 and (right) the difference with m1900 (m2000-m1900) in DJF, with light and dark shading indicating statistical significance at the 95% and 99% levels, respectively.

the eastward zonal winds at ~55–65°S. The changes in temperature in the SH upper mesosphere and lower thermosphere also suggest an upward shift of the mesopause. In the troposphere, there is a clear poleward shift of the midlatitude jet, accompanied by a significant cooling at high latitudes in the lower stratosphere and troposphere (70–90°S, 0–20 km) and a weaker warming around 50°S in the troposphere. The opposite temperature response is found in the middle stratosphere: Warming at high latitudes and cooling around 50–60°S. This quadrupole field of temperature anomalies is dynamically consistent with a positive Southern Annular Mode.

Significant differences are also found in the NH, but they are not zonally symmetric and therefore largely vanish in the zonal mean. Figure 4 illustrates this through a vertical cross section of the neutral temperature and meridional wind taken at 65°N, with longitude on the horizontal axis. The temperature differences in the middle atmosphere are clearly most pronounced in the Northern Atlantic-American sector (~0–90°W) and strongest around 60°W. A vertically alternating pattern of warming and cooling can be seen at this longitude. The upper atmosphere changes in temperature and wind are also strongest in this longitude sector (see Figure 2), because of the location of the NH magnetic pole near 80°W. However, it is not clear whether this is necessarily the reason for the stronger middle atmosphere responses in this region; it might also be related to zonal asymmetries in the background wind climatology in the NH middle atmosphere, which could perhaps favor a stronger response in this longitude sector, regardless of the longitudinal structure of the

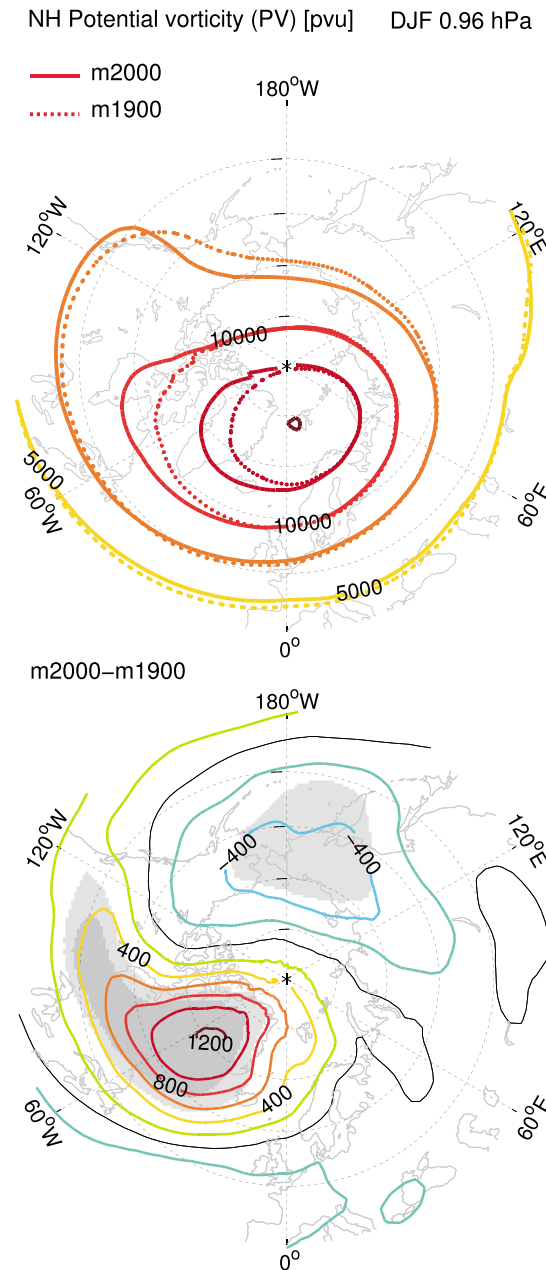


**Figure 5.** (top) Potential vorticity in the NH in potential vorticity units (pvu) at ~1 hPa for m2000 (solid lines) and m1900 (dotted lines) and (bottom) the difference (m2000-m1900) in DJF, with light and dark shading indicating statistical significance at the 95% and 99% levels, respectively.

[*Waugh and Randel, 1999; Harvey et al., 2002*]. It is also somewhat elongated in shape, and this is more pronounced in the m2000 case than the m1900 case. The elongation of the polar vortex occurs primarily toward the Atlantic-American sector (~0–90°W), resulting in a statistically significant increase in PV there for m2000 compared to m1900. There is a corresponding decrease in PV in the West Pacific sector (~150°W–120°E), which is weaker and less significant. Despite the difference in their strength, the positive and negative changes in PV mostly cancel out in a zonal mean.

Since significant changes in the structure and strength of the polar vortex are often related to the occurrence of major stratospheric sudden warming (SSW) events, one might expect a difference in the SSW occurrence

upper atmospheric forcing. The middle atmosphere meridional wind field exhibits a clear longitudinal structure in its climatology, tilting westward with height. It maximizes at ~50 km (~1 hPa), where winds blow northward between ~20°W and ~140°E, and southward at other longitudes. The m2000 climatology is in good agreement with observational climatologies of the longitudinal structure in meridional wind as shown by *Harvey and Hitchman [1996]* and *Kozubek et al. [2015]*. The m2000-m1900 difference indicates an intensification and slight westward shift of this structure.

*Kozubek et al. [2015]* explain that the longitudinal structure in the meridional wind in the NH winter stratosphere is associated with anticyclonic flow around the Aleutian High, typically located at ~180°E. The Aleutian High feature is often implicated in global forcing and teleconnection patterns and is closely related to the strength and positioning of the NH stratospheric polar vortex [e.g., *Harvey and Hitchman, 1996*, and references therein]. Because the NH polar vortex is generally not quite centered on the geographic pole, it cannot be properly visualized through the zonal mean zonal wind. The potential vorticity (PV) field is better suited to illustrate (the changes in) the positioning and shape of the polar vortex. The climatological PV at ~50 km and the associated m2000-m1900 difference from our simulations are shown in Figure 5.

In our simulations, the upper stratospheric polar vortex, characterized by high PV values, is displaced from the geographic pole, toward approximately 0° longitude, in good agreement with observational climatologies

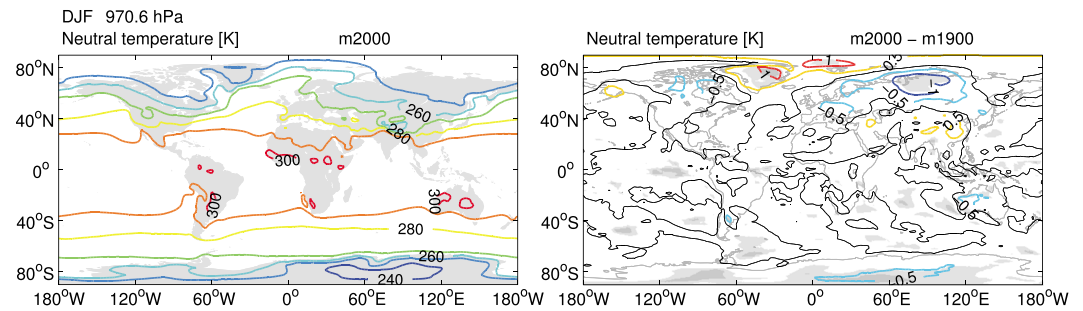


**Figure 6.** (left) Neutral temperature near the surface (970.6 hPa) for m2000 and (right) the difference with m1900 (m2000-m1900) in DJF, with light and dark shading indicating statistical significance at the 95% and 99% levels, respectively.

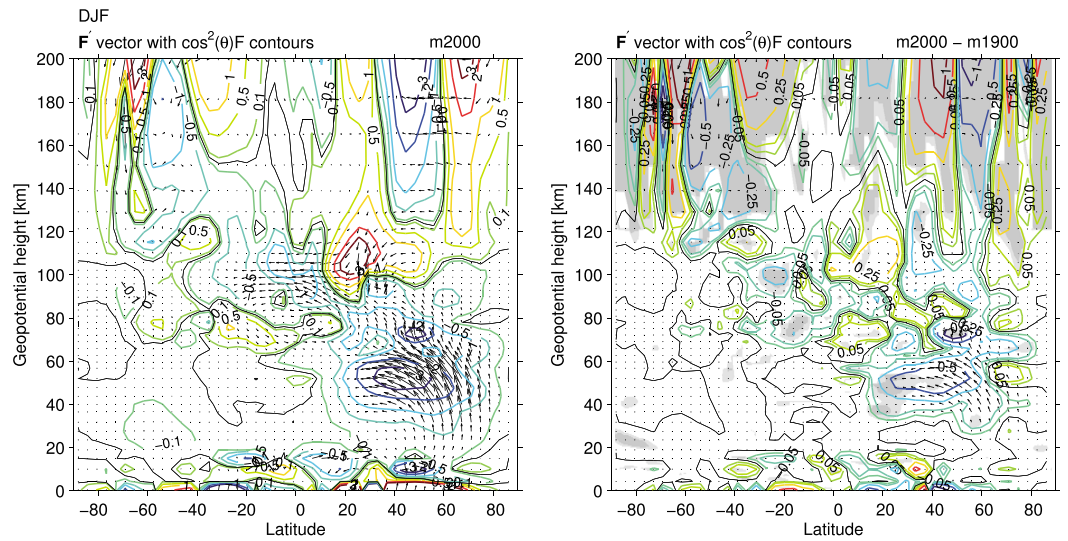
frequency between the m2000 and m1900 cases, which could potentially influence the average differences between our simulations. However, using the definition of *Charlton and Polvani* [2007] to identify major SSWs, we find that exactly the same number of events occurred in both simulations: 17 in 38 years. When we consider only SSW events in the DJF season, there are slightly more in the m1900 case (12) than in the m2000 case (10). We tested whether this difference has any effect on our results, by repeating the analysis with reduced data sets from which we excluded years in which an SSW occurred in DJF. This resulted in only minor changes in the patterns and the significance of the differences in temperature and zonal wind between our simulations as shown in Figure 3, although it did approximately double the magnitude of the differences in the NH stratosphere (not shown). We therefore conclude that the circulation differences shown in Figures 4 and 5 are not due to a change in SSW occurrence.

Figure 6 shows a map of the temperature differences near the surface, which are regionally significant, primarily at high latitudes, consistent with Figures 3 and 4. At SH high latitudes there is a decrease in temperature of up to 0.5 K, which is significant for most longitudes, but is strongest around 60°E. In the NH, there are small patches over Greenland and the Arctic Ocean that show a significant increase in temperature of up to 1.3 K, while a temperature decrease of up to 1.3 K is found over Siberia. This difference pattern looks similar to temperature anomalies associated with the negative phase of the Arctic Oscillation (AO) [Thompson and Wallace, 1998], which is known to be influenced by changes in both the tropospheric eddy-driven jet and the stratospheric polar vortex. The negative phase of the AO is normally associated with a weaker stratospheric vortex, while at least the absolute PV values as shown in Figure 5 indicate a stronger vortex for m2000. However, the vortex in the m2000 case is also more elongated and further displaced toward lower latitudes, giving rise to an enhanced wave-1 pattern. We suggest that it is these features, which are normally associated with a weaker vortex, which could be responsible for the AO-like pattern we find here in the surface temperature response.

#### 4. Possible Mechanisms for Downward Influence

The results presented in section 3 based on our simulations with WACCM-X indicate that changes in the thermosphere and ionosphere, initiated by the imposed magnetic field changes, are able to induce significant circulation changes in the mesosphere, stratosphere, and troposphere. This confirms similar findings from idealized modeling studies by *Arnold and Robinson* [1998, 2001, 2003]. In this section we will try to address the key question, namely, How does this work?

As noted in section 1, WACCM-X incorporates both the  $\text{NO}_x$ -ozone pathway and dynamical pathways of vertical atmospheric coupling. However, we found that the differences in  $\text{NO}_x$  and ozone between our simulations were small and statistically insignificant anywhere within the winter mesosphere or stratosphere, where the  $\text{NO}_x$ -ozone mechanism could play a role. This is understandable, as our simulations were run for low geomagnetic activity, when  $\text{NO}_x$  production is low. We can therefore rule out the  $\text{NO}_x$ -ozone pathway as an important contributor to the responses we find in the lower and middle atmosphere and will not study it hereafter. We will focus instead on dynamical pathways by which perturbations in the thermosphere may affect the atmosphere below.



**Figure 7.** (left) EP flux vector  $\mathbf{F}'$  (black arrows) and  $\cos^2(\theta)F$  (contours) for m2000 and (right) the difference with m1900 (m2000-m1900) in DJF calculated from seasonal mean data, with light and dark shading indicating statistical significance at the 95% and 99% levels, respectively. Contour levels are at 0,  $\pm 0.1$ ,  $\pm 0.5$ ,  $\pm 1$ ,  $\pm 2$ , and  $\pm 3$  m/s/d for m2000 and at 0,  $\pm 0.05$ ,  $\pm 0.25$ ,  $\pm 0.5$ , and  $\pm 1$  m/s/d for the difference.

We hypothesize that changes in the neutral wind structure in the lower thermosphere, produced directly by changes in the magnetic field, modify the conditions for wave propagation, thereby altering the wave forcing on the mean flow, which causes changes in the circulation at lower altitudes via the downward control principle [Haynes *et al.*, 1991]. Both resolved (planetary-scale) waves and parameterized gravity waves could be involved in this. We first investigate whether there are significant changes in (forcing by) resolved waves and gravity waves and then examine (changes in) the residual circulations they induce.

#### 4.1. Resolved Waves

The Eliassen-Palm (EP) flux is a standard diagnostic to examine the influence of planetary wave forcing on the mean flow [e.g., Andrews *et al.*, 1987]. We calculated EP flux diagnostics both from seasonal mean data for DJF, to emphasize the role of stationary waves, and from 5-daily data (data for every fifth day, the highest time resolution we have available for our simulations), which include contributions from both stationary and transient waves. Stationary waves are generally more important in the NH, while transient waves tend to be the main contributors to the wave forcing in the SH [Limpasuvan and Hartmann, 2000]. We note that the seasonal mean data are averaged over all universal times (UTs), whereas the 5-daily data are taken at 0 UT.

As we need to examine the atmosphere over a large vertical range, over which the standard EP flux varies by several orders of magnitude, we use a scaled version of the EP flux, following Chandran *et al.* [2013]:

$$\mathbf{F}' = (F'_\theta, F'_z) = \left( \frac{F_\theta \cos \theta}{\rho a}, \frac{F_z \cos \theta}{\rho a} \right) \quad (1)$$

where  $\mathbf{F} = (F_\theta, F_z)$  is the standard EP flux vector, consisting of components in the meridional ( $F_\theta$ ) and vertical ( $F_z$ ) direction,  $\theta$  is latitude,  $\rho$  is density, and  $a$  is the radius of the Earth. Figure 7 shows the vector  $\mathbf{F}'$  calculated from DJF mean data, with colored contours indicating the quantity  $\frac{\cos \theta}{\rho a} \nabla \cdot \mathbf{F}$ , called  $\cos^2(\theta)F$  by Chandran *et al.* [2013], which is a modified version of the standard EP flux divergence,  $\nabla \cdot \mathbf{F}$ , again because the standard EP flux divergence varies by several orders of magnitude across the vertical range we are interested in. We will refer to the vector  $\mathbf{F}'$  and the quantity  $\cos^2(\theta)F$ , simply as the EP flux (vector) and EP flux divergence in the remainder of the text. We note that similar results can be obtained by using monthly mean data (not shown).

The EP flux vectors and EP flux divergence shown in Figure 7 represent stationary wave contributions. In both the climatology and the difference plot, they are much larger in the NH middle atmosphere than in the SH. In the SH, we do note two patches of significant enhancements in EP flux divergence in the upper mesosphere and lower thermosphere around 15–25°S, which appear to be due to enhanced wave propagation from the NH into the SH (note the narrow channel around 20°N and ~85 km altitude in the climatology; Figure 7, left). The m2000-m1900 difference also shows significant enhancements in wave forcing (indicated by both negative EP flux divergence and enhanced upward and equatorward EP fluxes) around ~20°N at ~35–55 km in the stratosphere, on the equatorward side of the background climatology, and at ~50°N at ~70–75 km in the mesosphere, representing a strengthening of the local climatology there. Differences in the vertical EP flux component are mostly not significant, but differences in the horizontal EP flux component are significant between ~20°N and ~60°N at ~40–60 km altitude (not shown).

Standard EP flux diagnostics do not allow us to examine longitudinal variations in (changes in) wave propagation and forcing. However, *Plumb* [1985] showed that it is possible to generalize the EP theory to define a three-dimensional measure of the flux of wave activity, analogous to the EP flux (see also the more recent works by *Kinoshita et al.* [2010] and *Kinoshita and Sato* [2013]). Analysis of the *Plumb* [1985] flux showed that the strongest equatorward wave flux in the climatology at ~50 km altitude occurs in the Western Hemisphere between ~40°N and ~70°N. The m2000-m1900 shows an enhancement of this feature, with the strongest increase in equatorward wave flux occurring around 60°W (not shown). This is precisely where we found the strongest increase in potential vorticity (Figure 5). The same location also shows a small, but significant enhancement in upward wave flux. This result suggests enhanced wave refraction near the polar vortex edge where the eastward winds are strengthened, confirming a dynamic linkage between the changes in the polar vortex and the changes in resolved wave propagation. We suggest that it is most likely that the NH stratospheric response is initiated by a slight strengthening of the polar vortex, in particular around 60°W, with changes in wave propagation following as a consequence (if it were the other way around, enhanced wave forcing from the troposphere should have weakened the vortex, which is not what we find).

However, it is still unclear what caused the initial change in the polar vortex. There is not a clear connection between the responses we find in the stratosphere and mesosphere to those in the thermosphere. Even the enhancement in EP flux divergence at ~70–75 km altitude occurs at considerably lower altitude than the direct effects of the changes in the magnetic field on the wind and temperature structure, which only extend down to ~120 km altitude. Indeed, the EP flux vectors suggest that the mesospheric enhancement in EP flux divergence is actually due to enhanced upward wave propagation from the stratosphere below. Still, the responses in the stratosphere and mesosphere must somehow be initiated by a downward influence of the changes in the thermosphere.

We consider the possibility that changes in wave reflection in the lower thermosphere, due to changes in the vertical shear of the zonal mean zonal wind,  $\partial\bar{U}/\partial z$ , could produce an (apparently) disconnected response at much lower altitude. A negative zonal wind shear above a positive zonal wind shear acts as a barrier through which planetary waves cannot propagate, causing waves to be redirected [e.g., *Perlwitz and Harnik*, 2003, 2004]. Changes in the vertical structure of the zonal mean zonal wind can therefore cause changes in downward wave reflection. Figure 8 shows  $\partial\bar{U}/\partial z$  for DJF, indicating that there are indeed significant changes in the wind shear in the NH lower thermosphere (~100–120 km altitude) at high latitudes, which could potentially affect the propagation of planetary waves generated in the upper mesosphere/lower thermosphere region below. In the m2000 climatology there is a weakly positive zonal wind shear at ~100 km altitude with a weakly negative zonal wind shear above, which meets the condition for downward wave reflection. The m2000-m1900 difference shows an upward shift of this transition at the very highest latitudes (>80°N) and a downward shift around 70–75°N. Still, this on its own does not prove that any changes in wave reflection have necessarily occurred.

To check for further evidence for changes in wave reflection, we studied the zonal tilt of wave number –1, –2, and –3 structures. Upwardly propagating waves tilt westward with height, whereas downwardly propagating waves tilt eastward with height, so that an enhancement in downward wave reflection should result in a weaker westward tilt of the phase of the waves in a climatological average. However, we did not find any clear evidence of a significant change in the tilt of zonal wave number –1, –2, and –3 wave structures immediately below ~100–105 km altitude (not shown), where we found the significant change in  $\partial\bar{U}/\partial z$ . Our

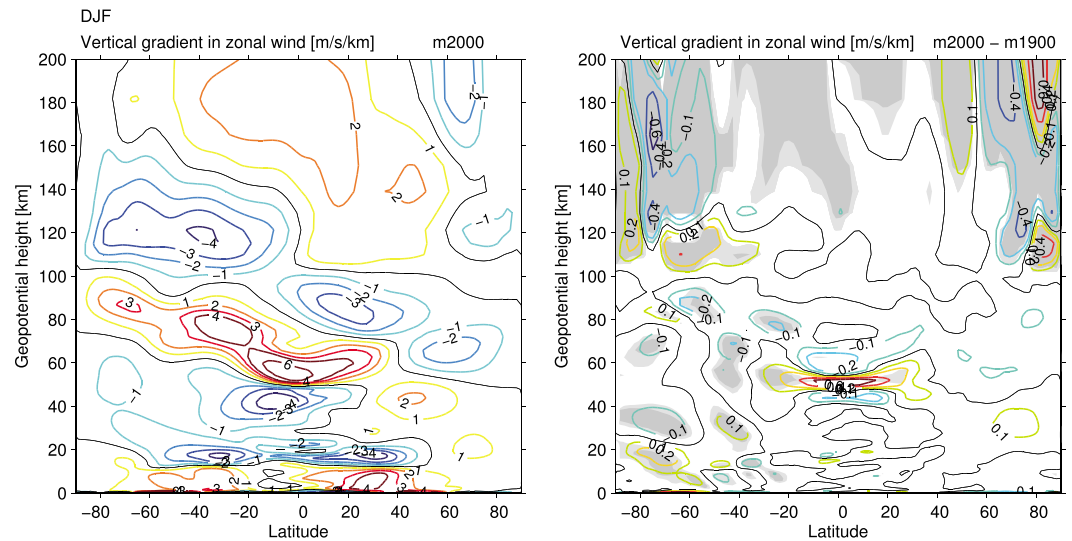


**Figure 8.** Vertical gradient of the zonal mean zonal wind,  $\partial\bar{U}/\partial z$ , for (left) m2000 and (right) the difference with m1900 (m2000-m1900) in DJF, with light and dark shading indicating statistical significance at the 95% and 99% levels, respectively.

analysis therefore suggests that a change in stationary planetary wave reflection may not be important for the downward communication of our wind anomalies in the thermosphere. Still, we cannot completely rule this mechanism out, as it may be a very subtle effect that is not properly captured by the model output data we have available.

Figure 9 shows the EP flux and EP flux divergence calculated from 5-daily data, with the contribution from the stationary waves as shown in Figure 7 removed. This therefore represents the propagation of and forcing by transient waves, which in the SH are more important, at least in the mesosphere (compare with Figure 7). We do note that we can only resolve relatively long-period transient waves, with periods of 10 days or longer, because we only have 5-daily data. Also, we only show results up to 100 km altitude, as the results at higher altitudes become extremely noisy and are not relevant here. In the NH stratosphere and lower mesosphere, there are a few small patches of positive change in EP flux divergence (at 70–85°N, 40–45 km; ~55–60°N, 60 km; ~45°N, 70–75 km; and ~30–35°N, 55–60 km). These occur in or on the edge of regions where the background climatology shows weakly positive EP flux divergence already, with EP flux vectors showing anomalous wave propagation away from the positive EP flux divergence region. This suggests enhanced wave generation within the midlatitude lower mesosphere. Similarly, in the SH upper mesosphere region, the m2000 climatology suggests that there are two regions of local wave generation, as indicated by positive

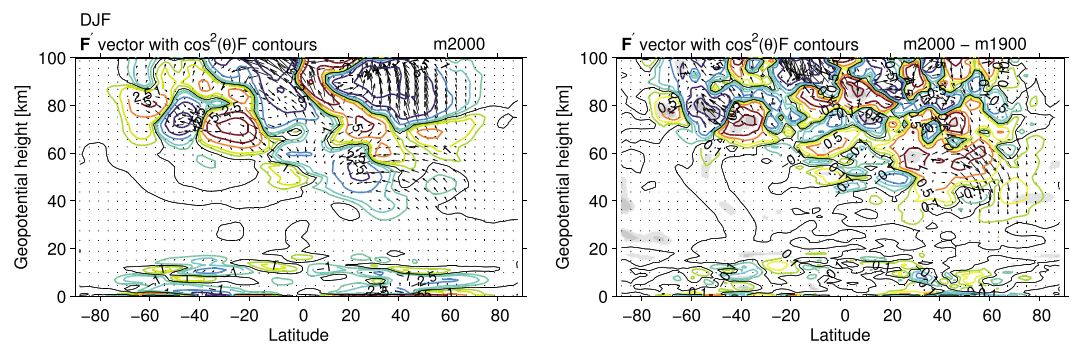


**Figure 9.** EP flux vector  $\mathbf{F}'$  (black arrows) and  $\cos^2(\theta)F$  (contours) for (left) m2000 and (right) the difference with m1900 (m2000-m1900) in DJF calculated from 5-daily data, with the contribution from stationary waves as shown in Figure 7 removed. Light and dark shading indicating statistical significance at the 95% and 99% levels, respectively. Contour levels are at 0,  $\pm 1$ ,  $\pm 2.5$ ,  $\pm 5$ ,  $\pm 10$ , and  $\pm 25$  m/s/d for m2000 and at 0,  $\pm 0.25$ ,  $\pm 0.5$ ,  $\pm 1$ ,  $\pm 2.5$ ,  $\pm 5$ , and  $\pm 10$  m/s/d for the m2000-m1900 difference.

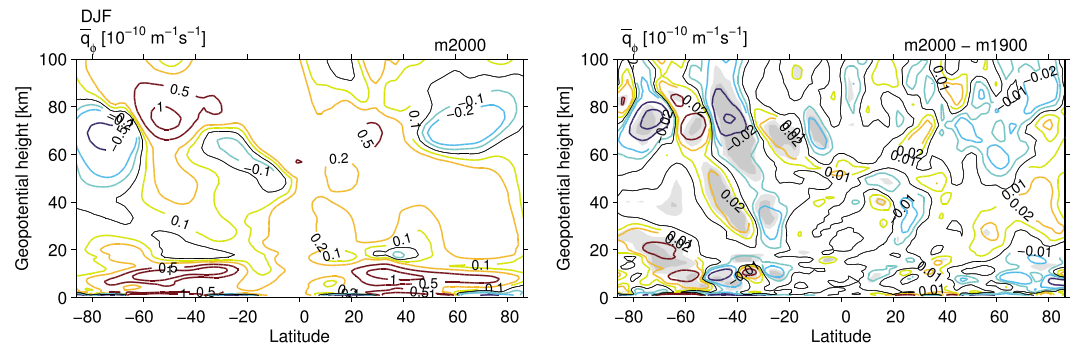


**Figure 10.** (left) Meridional PV gradient for m2000 and (right) the difference with m1900 (m2000-m1900) in DJF, with light and dark shading indicating statistical significance at the 95% and 99% levels, respectively. Contour levels are at 0,  $\pm 0.1$ ,  $\pm 0.2$ ,  $\pm 0.5$ , and  $\pm 1 \times 10^{-10} \text{ m}^{-1} \text{ s}^{-1}$  for m2000 and at 0,  $\pm 0.01$ ,  $\pm 0.02$ ,  $\pm 0.05$ , and  $\pm 0.1 \times 10^{-10} \text{ m}^{-1} \text{ s}^{-1}$  for the m2000-m1900 difference.

EP flux divergence, centered at  $\sim 60^\circ\text{S}$  and  $\sim 25^\circ\text{S}$ , with a region of wave dissipation in between, indicated by negative EP flux divergence. The EP flux vectors are consistent with this picture, showing waves propagating mostly horizontally away from the wave generation regions, leading to waves piling up in the region in between, where they dissipate. The m2000-m1900 shows primarily a poleward shift of this pattern, especially on the upper part of the pattern (the changes occur mainly above 70 km altitude). These changes in the resolved transient waves are likely to be associated with the changes in the zonal wind we saw in Figure 3.

Theoretical studies have shown that instabilities of the SH summertime mesospheric westward jet can generate or amplify waves in situ, such as the quasi 2 day wave [Plumb, 1983; Pfister, 1985; Ern et al., 2013; Vincent, 2015]. Instabilities can also form on the poleward and equatorward flanks of the eastward stratospheric vortex, where they are thought to interact with planetary waves propagating upward from the troposphere [Hartmann, 1983; Manney et al., 1991]. The periods of the waves that form on the equatorward flank of the vortex are on the order of a week or more, so that they can be captured by our 5-daily data, unlike the quasi 2 day wave in the SH mesosphere, or the waves that form on the poleward flank of the NH polar vortex, which tend to have periods of less than 4 days. While we can only partially diagnose the link between these unstable waves and the responses we find in the lower/middle atmosphere, we suggest that they could potentially play an important role in the vertical coupling mechanism. Further research will be needed to confirm (or disprove) this conjecture.

A necessary (though not sufficient) condition for instabilities to form is that the meridional PV gradient is negative. Figure 10 shows the meridional PV gradient,  $\bar{q}_p$ , for the m2000 case and the m2000-m1900 difference. In the NH stratosphere and mesosphere the changes in the meridional PV gradient are not statistically significant. However, we do see an enhancement of the region of negative PV gradient at  $40\text{--}90^\circ\text{N}$ ,  $70\text{--}90$  km altitude, which corresponds to the region that showed the strongest enhancement in positive EP flux divergence identified in Figure 9 (associated with transient waves). This suggests that the changes in EP flux divergence in the NH lower mesosphere may be associated with unstable waves. The region of positive EP flux divergence centered at  $\sim 25^\circ\text{S}$  at  $\sim 70$  km altitude in Figure 9 also corresponds closely to a region of negative meridional PV gradient in Figure 10, and another region of negative meridional PV gradient poleward of  $60^\circ\text{S}$  partially overlaps with a region of positive EP flux. This again strongly suggests that Rossby waves are being generated or amplified in these regions due to local instabilities of the mean flow. We cannot confirm from our data whether the main wave involved here is the quasi 2 day wave, which is known to be very important in the SH summer mesosphere [e.g., Ern et al., 2013; Vincent, 2015], because we cannot resolve it. Still, based on the studies mentioned above, it does seem likely that this wave is involved as well. The involvement of unstable waves in the upper mesosphere region in the downward propagation mechanism could further explain why we find that the strongest responses in the SH lower and middle atmosphere occur during DJF. Since the meridional PV gradient in the upper mesosphere can only become negative during summer [e.g., Plumb, 1983], local instabilities do not form there during other seasons. We suggest that this could make the downward propagation mechanism in the SH much less effective for seasons other than DJF.

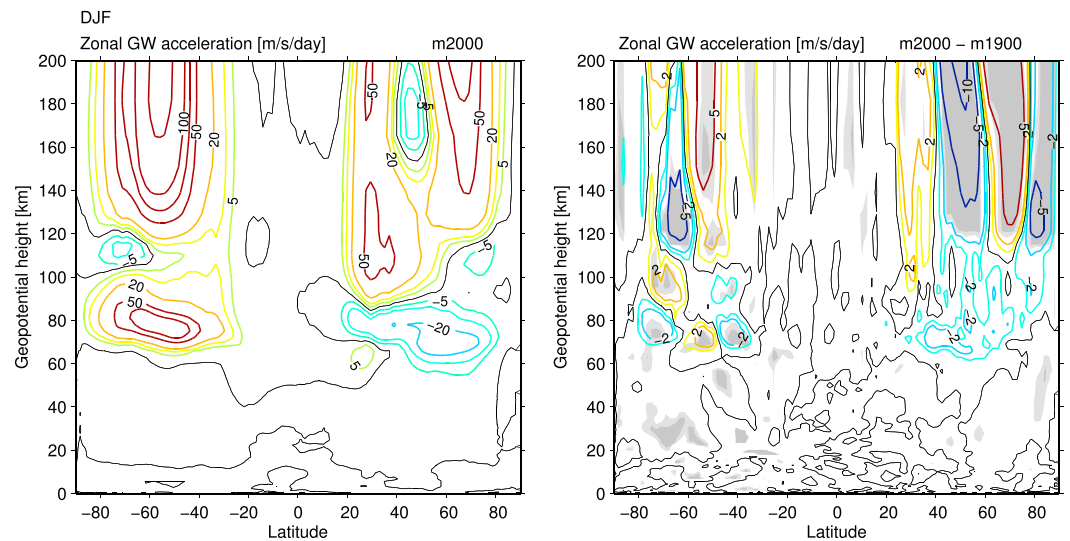


**Figure 11.** Zonal accelerations due to gravity waves for (left) m2000 case and (right) the difference with m1900 (m2000-m1900) with light and dark shading indicating statistical significance at the 95% and 99% levels, respectively. Contour levels are at  $\pm 5$ ,  $\pm 10$ ,  $\pm 20$ ,  $\pm 50$ ,  $\pm 75$ ,  $\pm 100$ , and  $\pm 150$  m/s/d for m2000 and  $\pm 1$ ,  $\pm 2$ ,  $\pm 5$ , and  $\pm 10$  m/s/d for the m2000-m1900 difference.

Both wave generation/amplification regions in the SH upper mesosphere are located just on the edge of the westward mesospheric jet (compare with Figure 3). This is relevant, because the formation of instabilities is closely related to the zonal wind curvature, and therefore the shape of the zonal jet [e.g., Pfister, 1985; Ern *et al.*, 2013]. Unfortunately, the “dip” in the zero-wind line at the top of the mesospheric jet that WACCM-X produces (at  $\sim 50$ – $55^\circ\text{S}$ ,  $\sim 70$  km altitude; see Figure 3) is not realistic (compare, e.g., to the observational climatology shown by Richter *et al.* [2008] in their Figure 1). Errors in the background wind structure are likely to lead to errors in the positioning and strength of wave generation/amplification regions in the SH upper mesosphere, which will then further interact with the mean wind climatology. Richter *et al.* [2008] performed a detailed assessment of the dynamics of the middle atmosphere as simulated by WACCM3 in comparison to observations, which demonstrated the same problem with the mesospheric jet that we find here with WACCM-X, as well as a quasi 2 day wave amplitude that was considerably smaller than seen in observations. It is highly likely that there are also problems with this wave in our simulations, and possibly with other unstable waves as well. This means that the changes in large-scale wave forcing we find in the SH upper mesosphere, as well as the changes in the zonal wind climatology in the same region, are not necessarily realistic and should be treated with suspicion. Nevertheless, the formation of baroclinic/barotropic instability in the summer mesopause region is reproduced reasonably in the model. We therefore do believe that the more general finding that this structure is sensitive to upper atmosphere changes and can influence the atmosphere below is valid, even though the details of the lower atmosphere response may not be correct.

#### 4.2. Parameterized Waves

In addition to resolved waves, the parameterized effects of sub-grid-scale gravity waves could play a role in communicating the upper atmosphere responses to the change in magnetic field to lower atmospheric layers. The (differences in) zonal forcing by gravity waves is shown in Figure 11. Nonorographic gravity wave forcing is generally stronger and therefore more important than orographic gravity wave forcing, and most of (the differences in) the accelerations shown in Figure 11 are associated with nonorographic gravity waves (based on separate analysis; not shown). We note that there is nearly no difference in gravity wave sources between the simulations (not shown) so the differences in gravity wave-induced accelerations come primarily from changes in filtering by the background winds. In the thermosphere this results very clearly in gravity wave-induced accelerations that are largely opposite in sign to the local changes in the zonal mean zonal wind.

In the NH middle atmosphere there is only a very small increase in the (eastward) zonal mean gravity wave forcing at high latitudes ( $\sim 80^\circ\text{N}$ ) in the stratopause region ( $\sim 50$  km,  $\sim 1$  hPa). This increase is strongly

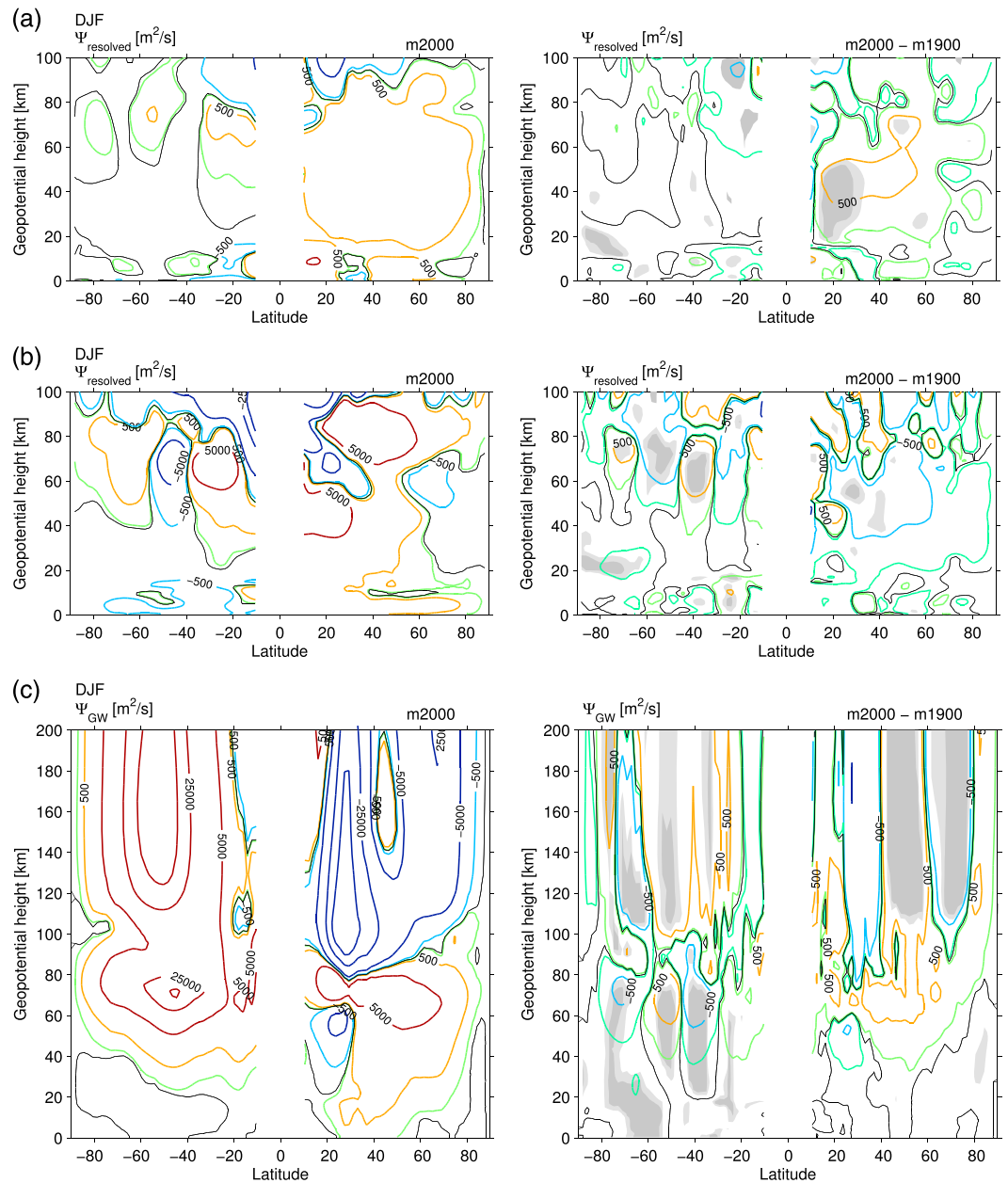


**Figure 12.** (a) Stream function of the DJF residual circulation for (left) m2000 and (right) the difference with m1900 (m2000-m1900) driven by stationary resolved waves, with light and dark shading indicating statistical significance at the 95% and 99% levels, respectively. Contour levels for both m2000 and the m2000-m1900 difference are 0,  $\pm 50$ ,  $\pm 500$ ,  $\pm 5000$ ,  $\pm 25000$ , and  $\pm 50000$   $m^2/s$ . (b) Stream function of the DJF residual circulation for (left) m2000 and (right) the difference with m1900 (m2000-m1900) driven by transient resolved waves, with light and dark shading indicating statistical significance at the 95% and 99% levels, respectively. Contour levels for both m2000 and the m2000-m1900 difference are the same as in Figure 12a. (c) Stream function of the DJF residual circulation for (left) m2000 and (right) the difference with m1900 (m2000-m1900) driven by parameterized gravity waves, with light and dark shading indicating statistical significance at the 95% and 99% levels, respectively. Contour levels for both m2000 and the m2000-m1900 difference are the same as in Figure 12a.

longitude dependent: Relatively enhanced eastward forcing is found mainly around 20–80°W at ~80°N (not shown). This particular longitude range corresponds quite well with the longitude range that showed the strongest increase in PV in Figure 5, indicating that this change in gravity wave forcing is associated with the change in the shape and positioning of the polar vortex.

In the SH middle atmosphere, we find an enhancement of eastward gravity wave forcing centered at  $\sim 50\text{--}55^\circ\text{S}$  and  $\sim 70\text{--}75$  km altitude, flanked by reductions in eastward forcing on either side. This corresponds closely to the difference pattern in the zonal wind (see Figure 3). We note that gravity wave forcing is also thought to be closely linked to instabilities of the mesospheric jet, which can generate or amplify waves, possibly seeding the horizontal curvature of the jet [e.g., *Pendlebury, 2012; Ern et al., 2013*]. Since gravity wave parameterizations are not perfect, there are likely to be errors in the gravity wave-induced accelerations in the model, which could be responsible for the unrealistic shape of the mesospheric jet in our simulations.

#### 4.3. Residual Circulation

Both resolved wave forcing and gravity wave forcing induce large-scale residual circulations, which couple remote parts of the atmosphere. We analyze these based on the downward control principle [*Haynes et al., 1991*], following *Okamoto et al.* [2011]. The stream functions associated with the residual circulations driven by different types of waves can be calculated using their equation (6):

$$\Psi(\theta, p) = \frac{\cos\theta}{g} \int_p^0 \frac{\overline{\mathcal{F}}}{\widehat{f}} dp' \quad (2)$$

where  $g$  is the gravitational acceleration,  $p$  is pressure,  $\overline{\mathcal{F}}$  is a zonal force,  $\widehat{f} = f - \frac{\partial(\bar{u} \cos\theta)/\partial\theta}{a \cos\theta}$ ,  $\bar{u}$  is the zonal mean zonal wind, and  $f$  the Coriolis parameter. By substituting for  $\overline{\mathcal{F}}$  either the resolved wave forcing associated with stationary or transient waves (i.e., the unscaled EP flux divergence; see Figures 7 and 9, except scaled versions are shown) or the gravity wave forcing, we calculated the residual circulations associated with these waves, shown in Figures 12a–12c. A latitude band of  $10^\circ$  within the equator has been left blank, because  $\widehat{f}$  tends to zero in the tropics, making the analysis invalid for low latitudes. We only show the residual circulation driven by resolved waves up to 100 km, as they do not play an important role at higher altitudes.

The residual circulation driven by gravity waves (Figure 12c) shows widespread significant changes, in both the thermosphere (in both hemispheres) and the atmosphere below (in the SH only). In the SH, there is a deep gravity wave-induced residual circulation cell that extends from the thermosphere down into the mesosphere and stratosphere. We suggest that it is most likely that the initial communication of changes in the wind structure in the thermosphere down to the upper mesosphere region occurs via changes to this residual circulation cell, driven by changes in gravity wave forcing in the thermosphere due to changes in wave filtering by the mean wind. This will drive a response in the upper mesosphere mean wind, which then further affects local planetary wave activity and gravity wave filtering and forcing.

The pattern of alternating positive and negative changes in gravity wave forcing in the SH upper mesosphere, which we discussed above, has a downward influence that can be seen to extend all the way into the troposphere. This strongly suggests that gravity wave forcing also plays an important role in inducing the responses we find in the SH troposphere and stratosphere. However, the changes in gravity wave forcing in the SH upper mesosphere region clearly occur in close conjunction with the local changes in the mean wind and the (transient) planetary wave forcing, which, as we have already discussed, are likely to be unrealistic. Thus, it is best to treat the SH response with caution. Nevertheless, even though the reliability of the responses we find in the SH lower and middle atmosphere may be questionable, the physical mechanisms by which these responses arise in the model are still valid.

In the NH, gravity wave forcing is less important, and changes in the gravity wave-induced residual circulation are mostly confined to the thermosphere. There are significant changes in the residual circulation forced by both stationary and transient resolved waves in the NH stratosphere. Enhanced stationary wave forcing at low latitudes has caused a local strengthening of the residual circulation at  $\sim 15\text{--}30^\circ\text{N}$  and 20–50 km altitude, while changes in transient wave forcing at  $\sim 30\text{--}40^\circ\text{N}$  and 40–60 km altitude have acted mostly in the opposite direction, weakening the residual circulation. Again though, the connection between the thermosphere and stratosphere is unclear.

## 5. Discussion and Conclusions

We have demonstrated through simulations with WACCM-X that changes in the Earth's magnetic field from 1900 to 2000, which directly affect the ionosphere and thermosphere, can cause further, indirect changes in the atmosphere below, in particular during DJF. In the SH, there are significant changes in zonal mean

temperature and zonal mean zonal winds of up to  $\pm 2$  K and  $\pm 2$  m/s, respectively, throughout large portions of the troposphere, stratosphere, and mesosphere. In the NH, there is no significant zonal mean change, but there is a significant change in the positioning and shape of the stratospheric polar vortex, in particular over the Atlantic region. Near the surface, there are regionally significant changes in NH temperature over Greenland and the Arctic Ocean (up to +1.3 K) and over Siberia (up to  $-1.3$  K). Based on our analysis, we suggest that the changes in the lower and middle atmosphere arise as follows.

The movement of the magnetic poles between 1900 and 2000 directly affects the zonal mean zonal wind structure in the thermosphere, changing the local conditions for wave propagation and breaking. This causes changes to zonal gravity wave-induced accelerations within the thermosphere and to the residual circulation driven by these accelerations. Because this residual circulation extends downward from the forcing region, the effects of changes in gravity wave forcing in the thermosphere are able to reach down to the mesosphere below, at least in the SH. We believe that this is the most likely mechanism by which changes in the SH upper mesosphere are initiated.

An initial change in the zonal wind structure in the SH upper mesosphere induces further changes in both planetary waves, which can be locally generated or amplified due to instabilities forming on the upper part of the westward mesospheric jet, and gravity wave filtering, both of which cause further changes to the zonal wind structure, which further affects the waves, and so on. The net changes in the gravity wave forcing within the upper mesosphere region itself cause changes in the gravity wave-induced residual circulation that extend down to the troposphere. We suggest that this is likely to initiate again further changes in the zonal mean zonal wind structure and planetary waves there.

While this mechanism can explain why we see such widespread significant changes in temperature and zonal wind in the SH lower and middle atmosphere in our model results, we do not necessarily believe that these changes are realistic, because the simulated shape of the mesospheric jet in the SH shows a dip in its structure at  $\sim 50$ – $55^\circ$ S that is not seen in observations. The shape of the mesospheric jet is very important for the formation of instabilities that can generate or amplify planetary-scale waves in the upper mesosphere region, and since this region appears to play a critical role in the vertical coupling in the SH, we must question the realism of the changes in zonal mean temperature and zonal wind we obtain throughout the SH troposphere, stratosphere, and mesosphere. Improvements to the SH zonal wind climatology produced by WACCM-X are needed to resolve this issue. A better representation of effects of sub-grid-scale gravity waves in WACCM-X would probably play an important role in this.

In the NH, gravity waves induce a residual circulation cell in the thermosphere that is separate from the mesosphere, and significant changes in the gravity wave-induced residual circulation are mostly confined to the thermosphere. This could potentially explain why we see much less significant change in the NH lower and middle atmosphere. Still, we do find a significant change in the shape and positioning of the stratospheric polar vortex, indicating that there is some vertical coupling process that allows the NH stratosphere to respond to a change in the thermosphere. We are not able to tell from our results whether this process involves perhaps a very subtle change in the gravity wave-driven residual circulation, or whether there is perhaps a subtle change in resolved wave reflection in the lower thermosphere due to a change in the vertical gradient of the zonal mean zonal wind. It is also possible that unstable waves that form on the upper part of the polar vortex play a role in the responses we find in the NH lower mesosphere and upper stratosphere, although changes in EP flux diagnostics and meridional PV gradient were mostly not significant in the NH. This lack of significance might be related to zonal asymmetries and the influence of stationary waves contaminating the signal in the NH. We further note that it is intriguing that the longitude sector that shows the strongest changes in the NH stratosphere is also the longitude sector that contains the NH magnetic pole, which moved westward by about  $3^\circ$  between 1900 and 2000. However, it is not clear whether this has any special significance or is merely a coincidence. We do not see a similar longitudinal preference of the lower and middle atmosphere response in the SH, even though the response in the SH upper atmosphere does show strong longitudinal variations, which are, as in the NH, related to the movement of the magnetic pole.

Changes in the polar vortex in the stratosphere are able to have a downward influence on the temperatures near the surface. A strong stratospheric polar vortex acts to confine cold air to the polar region, whereas a weaker stratospheric polar vortex allows colder air to get into lower latitude regions. A strong polar vortex is therefore associated with a positive phase of the AO near the surface [e.g., Baldwin and Dunkerton,

1999]. We find a difference pattern in NH surface temperature that resembles the negative phase of the AO, with warming over Greenland and the Arctic Ocean and cooling over Siberia, even though the (upper) stratospheric vortex in our simulations showed a slight strengthening. However, the vortex in our simulations was also more elongated in shape and further displaced toward lower latitudes. We believe that these aspects, which are normally associated with a weaker vortex, could be responsible for the NH surface temperature response in our simulations.

The NH differences near the surface suggest that a change in the Earth's magnetic field does not necessarily produce a uniform increase or decrease in temperature. This could perhaps explain some of the discrepancies between the correlation studies mentioned in the introduction: One might find that an overall decrease in magnetic field strength, as has taken place during the last ~170 years, is associated with either an increase or decrease in surface temperature, depending on the geographic origin of the temperature (or temperature proxy) data that are used. Interestingly, the finding by *Bakhtmutov* [2006] that temperatures in Northeastern Europe were typically 1–2 K higher as the geomagnetic pole was approaching the region and 1–2 K lower as it was receding from the region, appears to be confirmed by our results: From 1900 to 2000 the geomagnetic pole was moving toward Northeastern Europe, and we indeed find a cooling in that region of 1–1.3 K. However, our result is of course based on only one example of a magnetic pole movement, and the correspondence with *Bakhtmutov* [2006] could be a coincidence. Further work is needed to determine how important the precise location and direction of movement of the magnetic pole is for determining the structure and magnitude of the temperature responses near the surface.

We further stress that our model simulations do not incorporate all possible mechanisms by which changes in the upper atmosphere could conceivably affect the middle and lower atmosphere, as outlined in section 1. It would be possible to test with the current version of WACCM-X what the role of the NO<sub>x</sub>-ozone mechanism is when geomagnetic activity is higher, but this falls outside the scope of the present study. Further model development is needed to be able to study also other possible coupling mechanisms, such as via the global electric circuit. Nonetheless, our results here show that dynamical mechanisms alone are capable of inducing a response in the lower and middle atmosphere to a forcing that does not have a direct effect in those parts of the atmosphere. While we have focused here on the downward influence of changes in the thermosphere that are associated with changes in the Earth's magnetic field, other processes that cause significant perturbations in the lower thermosphere could in principle affect the atmosphere below via similar pathways.

#### Acknowledgments

This study is part of the British Antarctic Survey Polar Science for Planet Earth Programme. I. Cnossen was sponsored by a fellowship of the Natural Environment Research Council, grant NE/J018058/1. H.-L. Liu acknowledges support by National Science Foundation grant AGS-1138784 and NASA LWS NNX16AB82G and NNX14AH54G. The WACCM-X simulations were performed on the Yellowstone high-performance computing facility (ark:/85065/d7wd3xhc) provided by the Computational and Information Systems Laboratory of the National Centre for Atmospheric Research, sponsored by the National Science Foundation. Modeling results will be made freely available to the scientific community on request (contact I. Cnossen; inos@bas.ac.uk; icnossen@yahoo.com).

#### References

- Andrews, D. G., J. R. Holton, and C. B. Leovy (1987), *Middle Atmosphere Dynamics*, Academic Press, London.
- Arnold, N. F., and T. R. Robinson (1998), Solar cycle changes to planetary wave propagation and their influence on the middle atmosphere circulation, *Ann. Geophys.*, *16*, 69–76.
- Arnold, N. F., and T. R. Robinson (2001), Solar magnetic flux influences on the dynamics of the winter middle atmosphere, *Geophys. Res. Lett.*, *28*, 2381–2384, doi:10.1029/2000GL012825.
- Arnold, N. F., and T. R. Robinson (2003), Solar cycle modulation of the winter stratosphere: The role of atmospheric gravity waves, *Adv. Space Res.*, *31*(9), 2121–2126.
- Badhwar, G. D. (1997), Drift rate of the South Atlantic Anomaly, *J. Geophys. Res.*, *102*, 2343–2349, doi:10.1029/96JA03494.
- Bakhtmutov, V. (2006), The connection between geomagnetic secular variation and long-range development of climate changes for the last 13,000 years: The data from NNE Europe, *Quat. Int.*, *149*, 4–11.
- Baldwin, M. P., and T. J. Dunkerton (1999), Propagation of the Arctic Oscillation from the stratosphere to the troposphere, *J. Geophys. Res.*, *104*, 30,937–30,946.
- Baldwin, M. P., and T. J. Dunkerton (2001), Stratospheric harbingers of anomalous weather regimes, *Science*, *294*, 581–584, doi:10.1126/science.1063315.
- Baumgaertner, A. J. G., A. Seppälä, P. Jöckel, and M. A. Clilverd (2011), Geomagnetic activity related NO<sub>x</sub> enhancements and polar surface air temperature variability in a chemistry climate model: Modulation of the NAM index, *Atmos. Chem. Phys.*, *11*, 4521–4531.
- Baumgaertner, A. J. G., J. P. Thayer, R. R. Neely III, and G. Lucas (2013), Towards a comprehensive global electric circuit model: Atmospheric conductivity and its variability in CESM1(WACCM) model simulations, *J. Geophys. Res. Atmos.*, *118*, 9221–9232, doi:10.1002/jgrd.50725.
- Chandran, A., R. R. Garcia, R. L. Collins, and L. C. Chang (2013), Secondary planetary waves in the middle and upper atmosphere following the stratospheric sudden warming event of January 2012, *Geophys. Res. Lett.*, *40*, 1861–1867, doi:10.1002/grl.50373.
- Charlton, A. J., and L. M. Polvani (2007), A new look at stratospheric sudden warmings. Part I: Climatology and modelling benchmarks, *J. Clim.*, *20*, 449–469.
- Christiansen, B. (2001), Downward propagation of zonal mean zonal wind anomalies from the stratosphere to the troposphere: Model and reanalysis, *J. Geophys. Res.*, *106*, 27,307–27,322, doi:10.1029/2000JD000214.
- Cnossen, I. (2014), The importance of geomagnetic field changes versus rising CO<sub>2</sub> levels for long-term change in the upper atmosphere, *J. Space Weather Space Clim.*, *4*, 8, doi:10.1051/swsc/2014016.
- Cnossen, I., and A. D. Richmond (2008), Modelling the effects of changes in the Earth's magnetic field from 1957 to 1997 on the ionospheric  $h_mF_2$  and  $f_oF_2$  parameters, *J. Atmos. Sol. Terr. Phys.*, *70*, 1512–1524.

- Cnossen, I., and A. D. Richmond (2012), How changes in the tilt angle of the geomagnetic dipole affect the coupled magnetosphere-ionosphere-thermosphere system, *J. Geophys. Res.*, *117*, A10317, doi:10.1029/2012JA018056.
- Cnossen, I., and A. D. Richmond (2013), Changes in the Earth's magnetic field over the past century: Effects on the ionosphere-thermosphere system and solar quiet (Sq) magnetic variation, *J. Geophys. Res. Space Physics*, *118*, 1–10, doi:10.1029/2012JA018447.
- Cnossen, I., A. D. Richmond, M. Wiltberger, W. Wang, and P. Schmitt (2011), The response of the coupled magnetosphere-ionosphere-thermosphere system to a 25% reduction in the dipole moment of the Earth's magnetic field, *J. Geophys. Res.*, *116*, A12304, doi:10.1029/2011JA017063.
- Cnossen, I., A. D. Richmond, and M. Wiltberger (2012a), The dependence of the coupled magnetosphere-ionosphere-thermosphere system on the Earth's magnetic dipole moment, *J. Geophys. Res.*, *117*, A05302, doi:10.1029/2012JA017555.
- Cnossen, I., M. Wiltberger, and J. E. Ouellette (2012b), The effects of seasonal and diurnal variations in the Earth's magnetic dipole orientation on solar wind-magnetosphere-ionosphere coupling, *J. Geophys. Res.*, *117*, A11211, doi:10.1029/2012JA017825.
- Courtillet, V., Y. Gallet, J.-L. Le Mouél, F. Fluteau, and A. Genevey (2007), Are there connections between the Earth's magnetic field and climate?, *Earth Plan. Sci. Lett.*, *253*, 328–339.
- De Santis, A., E. Qamili, G. Spada, and P. Gasperini (2012), Geomagnetic South Atlantic Anomaly and global seas level rise: A direct connection?, *J. Atmos. Sol. Terr. Phys.*, *74*, 129–135.
- Ern, M., P. Preuse, S. Kalisch, M. Kaufmann, and M. Riese (2013), Role of gravity waves in the forcing of quasi two-day waves in the mesosphere: An observational study, *J. Geophys. Res. Atmos.*, *118*, 3467–3485, doi:10.1029/2012JD018208.
- Finlay, C. C., et al. (2010), International Geomagnetic Reference Field: The eleventh generation, *Geophys. J. Int.*, *183*, 1216–1230.
- Fritts, D. C., and M. J. Alexander (2003), Gravity wave dynamics and effects in the middle atmosphere, *Rev. Geophys.*, *41*(1), 1003, doi:10.1029/2001RG000106.
- Funke, B., M. López-Puertas, D. Bermejo-Pantaleón, et al. (2010), Evidence for dynamical coupling from the lower atmosphere to the thermosphere during a major stratospheric warming, *Geophys. Res. Lett.*, *37*, L13803, doi:10.1029/2010GL043619.
- Gallet, Y., A. Genevey, and F. Fluteau (2005), Does Earth's magnetic field secular variation control centennial climate change?, *Earth Plan. Sci. Lett.*, *236*, 339–347.
- García, R. R., D. R. Marsh, D. E. Kinnison, B. A. Boville, and F. Sassi (2007), Simulation of secular trends in the middle atmosphere, 1950–2003, *J. Geophys. Res.*, *112*, D09301, doi:10.1029/2006JD007485.
- Gubbins, D., A. L. Jones, and C. C. Finlay (2006), Fall in Earth's magnetic field is erratic, *Science*, *312*, 900–902.
- Hartmann, D. L. (1983), Barotropic instability of the polar night jet stream, *J. Atmos. Sci.*, *40*(4), 817–835.
- Harvey, V. L., and M. H. Hitchman (1996), A climatology of the Aleutian High, *J. Atmos. Sci.*, *53*, 2088–2101.
- Harvey, V. L., R. B. Pierce, T. D. Fairlie, and M. H. Hitchman (2002), A climatology of stratospheric polar vortices and anticyclones, *J. Geophys. Res.*, *107*(D20), 4442, doi:10.1029/2001JD001471.
- Haynes, P. H., C. J. Marks, M. E. McIntyre, T. G. Shepherd, and K. P. Shine (1991), On the “downward control” of extratropical diabatic circulations by eddy-induced mean zonal forces, *J. Atmos. Sci.*, *48*(4), 651–678.
- Hines, C. O. (1974), A possible mechanism for the production of Sun-weather correlations, *J. Atmos. Sci.*, *31*, 589–591.
- Holton, J. R. (1984), The generation of mesospheric planetary waves by zonally asymmetric gravity wave breaking, *J. Atmos. Sci.*, *41*, 3427–3430.
- King, J. W. (1975), Sun-weather relationships, *Aeronautics Astronautics*, *13*(4), 10–19.
- Kinoshita, T., and K. Sato (2013), A formulation of unified three-dimensional wave activity flux of inertia-gravity waves and Rossby waves, *J. Atmos. Sci.*, *70*, 1603–1615.
- Kinoshita, T., Y. Tomikawa, and K. Sato (2010), On the three-dimensional residual mean circulation and wave activity flux of the primitive equations, *J. Meteor. Soc. Jpn.*, *88*, 373–394.
- Kitaba, I., M. Hyodo, S. Katoh, D. L. Dettman, and H. Sato (2013), Midlatitude cooling caused by geomagnetic field minimum during polarity reversal, *Proc. Natl. Acad. Sci. U.S.A.*, *110*(4), 1215–1220.
- Knudsen, M. F., and P. Riisager (2009), Is there a link between Earth's magnetic field and low-latitude precipitation?, *Geology*, *37*(1), 71–74.
- Kozubek, M., P. Krizan, and J. Laštovička (2015), Northern hemisphere stratospheric winds in higher midlatitudes: Longitudinal distribution and long-term trends, *Atmos. Chem. Phys.*, *15*, 2203–2213.
- Laken, B. A., E. Pallé, J. Čalogović, and E. M. Dunne (2012), A cosmic ray-climate link and cloud observations, *J. Space Weather Space Clim.*, *2*, A18.
- Lam, M. M., G. Chisham, and M. P. Freeman (2013), The interplanetary magnetic field influences mid-latitude surface atmospheric pressure, *Environ. Res. Lett.*, *8*, doi:10.1088/1748-9326/8/4/045001.
- Lam, M. M., G. Chisham, and M. P. Freeman (2014), Solar wind-driven geopotential height anomalies originate in the Antarctic lower troposphere, *Geophys. Res. Lett.*, *41*, 6509–6514, doi:10.1002/2014GL061421.
- Limpasuvan, V., and D. L. Hartmann (2000), Wave-maintained annular modes of climate variability, *J. Clim.*, *13*, 4414–4429.
- Liu, H.-L., et al. (2010), Thermosphere extension of the Whole Atmosphere Community Climate Model, *J. Geophys. Res.*, *115*, A12302, doi:10.1029/2010JA015586.
- Lu, H., M. A. Clilverd, A. Seppälä, and L. L. Hood (2008), Geomagnetic perturbations on stratospheric circulation in late winter and spring, *J. Geophys. Res.*, *113*, D16106, doi:10.1029/2007JD008915.
- Mandea, M., and M. Purucker (2005), Observing, modelling, and interpreting magnetic fields of the solid Earth, *Surv. Geophys.*, *26*, 415–459.
- Manney, G. L., C. R. Mechoso, L. S. Elson, and J. D. Farrara (1991), Planetary-scale waves in the southern hemisphere winter and early spring stratosphere: Stability analysis, *J. Atmos. Sci.*, *48*, 2509–2523.
- Mayr, H. G., J. G. Mengel, E. R. Talaat, H. S. Porter, and K. L. Chan (2004), Modeling study of mesospheric planetary waves: Genesis and characteristics, *Ann. Geophys.*, *22*, 1885–1902.
- Newitt, L. R., M. Mandea, L. A. McKee, and J.-J. Orgeval (2002), Recent acceleration of the north magnetic pole linked to magnetic jerks, *Eos Trans. AGU*, *83*(35), 381–389, doi:10.1029/2002EO000276.
- Okamoto, K., K. Sato, and H. Akiyoshi (2011), A study on the formation and trend of the Brewer-Dobson circulation, *J. Geophys. Res.*, *116*, D10117, doi:10.1029/2010JD014953.
- Olsen, N., and M. Mandea (2007), Will the magnetic North pole move to Siberia?, *Eos Trans. AGU*, *88*(29), 293–300, doi:10.1029/2007EO290001.
- Pendlebury, D. (2012), A simulation of the quasi-two-day wave and its effects on variability of summertime mesopause temperatures, *J. Atmos. Sol. Terr. Phys.*, *80*, 138–151.
- Perlwitz, J., and N. Harnik (2003), Observational evidence for a stratospheric influence on the troposphere by planetary wave reflection, *J. Clim.*, *16*, 3011–3026.

- Perlwitz, J., and N. Harnik (2004), Downward coupling between the stratosphere and troposphere: The relative roles of wave and zonal mean processes, *J. Clim.*, *17*, 4902–4909.
- Pfister, L. (1985), Baroclinic instability of easterly jets with applications to the summer mesosphere, *J. Atmos. Sci.*, *42*(4), 313–330.
- Plumb, R. A. (1983), Baroclinic instability of the summer mesosphere: A mechanism for the quasi-two-day wave?, *J. Atmos. Sci.*, *40*, 262–270.
- Plumb, R. A. (1985), On the three-dimensional propagation of stationary waves, *J. Atmos. Sci.*, *42*, 217–229.
- Randall, C. E., V. L. Harvey, C. S. Singleton, S. M. Bailey, P. F. Bernath, M. Codrescu, H. Nakajima, and J. M. Russell III (2007), Energetic particle precipitation effects on the Southern hemisphere stratosphere in 1992–2005, *J. Geophys. Res.*, *112*, D08308, doi:10.1029/2006JD007696.
- Randall, C. E., V. L. Harvey, L. A. Holt, D. R. Marsh, D. Kinnison, B. Funke, and P. F. Bernath (2015), Simulation of energetic particle precipitation effects during the 2003–2004 Arctic winter, *J. Geophys. Res. Space Physics*, *120*, 5035–5048, doi:10.1002/2015JA021196.
- Richmond, A. D. (1995), Ionospheric electrodynamics using magnetic apex coordinates, *J. Geomag. Geoelectr.*, *47*, 191–212.
- Richter, J. H., F. Sassi, R. R. Garcia, K. Matthes, and C. A. Fischer (2008), Dynamics of the middle atmosphere as simulated by the Whole Atmosphere Community Climate Model, version 3 (WACCM3), *J. Geophys. Res.*, *113*, D08101, doi:10.1029/2007JD009269.
- Richter, J. H., F. Sassi, and R. R. Garcia (2010), Towards a physically based gravity wave source parameterization in a general circulation model, *J. Atmos. Sci.*, *67*, 136–156.
- Rishbeth, H. (1984), The quadrupole ionosphere, *Ann. Geophys.*, *3*, 293–298.
- Roble, R. G., and E. C. Ridley (1987), An auroral model for the NCAR thermosphere general circulation model (TGCM), *Ann. Geophys.*, *5A*, 369–382.
- Seppälä, A., M. A. Clilverd, and C. J. Rodger (2007), NO<sub>x</sub> enhancements in the middle atmosphere during 2003–2004 polar winter: Relative significance of solar proton events and the aurora as a source, *J. Geophys. Res.*, *112*, D23303, doi:10.1029/2006JD008326.
- Seppälä, A., H. Lu, M. A. Clilverd, and C. J. Rodger (2013), Geomagnetic activity signatures in wintertime stratosphere wind, temperature, and wave response, *J. Geophys. Res. Atmos.*, *118*, 2169–2183, doi:10.1002/jgrd.50236.
- Smith, A. K. (2003), The origin of stationary planetary waves in the upper mesosphere, *J. Atmos. Sci.*, *60*, 3033–3041.
- Solomon, S., P. J. Crutzen, and R. G. Roble (1982), Photochemical coupling between the thermosphere and lower atmosphere: 1. Odd nitrogen from 50 to 120 km, *J. Geophys. Res.*, *87*, 7206–7220, doi:10.1029/JC087iC09p07206.
- Takeda, M. (1996), Effects of the strength of the geomagnetic main field strength on the dynamo action in the ionosphere, *J. Geophys. Res.*, *101*, 7875–7880, doi:10.1029/95JA03807.
- Thompson, D. W. J., and J. M. Wallace (1998), The Arctic Oscillation signature in the wintertime geopotential height and temperature fields, *Geophys. Res. Lett.*, *25*, 1297–1300, doi:10.1029/98GL00950.
- Thompson, D. W. J., M. P. Baldwin, and J. M. Wallace (2002), Stratospheric connection to Northern hemisphere wintertime weather: Implications for prediction, *J. Clim.*, *15*, 1421–1428.
- Thompson, D. W. J., M. P. Baldwin, and S. Solomon (2005), Stratosphere-troposphere coupling in the southern hemisphere, *J. Atmos. Sci.*, *62*, 708–715.
- Tinsley, B. A. (2008), The global atmospheric electric circuit and its effect on cloud microphysics, *Rep. Prog. Phys.*, *71*(6), 066801, doi:10.1088/0034-4885/71/6/066801.
- Vadas, S. L., and H. L. Liu (2009), Generation of large-scale gravity waves and neutral winds in the thermosphere from the dissipation of convectively generated gravity waves, *J. Geophys. Res.*, *114*, A10310, doi:10.1029/2009JA014108.
- Vieira, L. E. A., L. A. da Silva, and F. L. Guarnieri (2008), Are changes of the geomagnetic field intensity related to changes of the tropical Pacific sea-level pressure during the last 50 years?, *J. Geophys. Res.*, *113*, A08226, doi:10.1029/2008JA013052.
- Vincent, R. A. (2015), The dynamics of the mesosphere and lower thermosphere: A brief review, *Prog. Earth. Planetary Sci.*, *2*, 4, doi:10.1186/s40645-015-0035-8.
- Waugh, D. W., and W. J. Randel (1999), Climatology of Arctic and Antarctic polar vortices using elliptical diagnostics, *J. Atmos. Sci.*, *56*, 1594–1613.
- Weimer, D. T. (1996), A flexible, IMF dependent model of high-latitude electric potentials having “space weather” applications, *Geophys. Res. Lett.*, *23*, 2549–2552, doi:10.1029/96GL02255.
- Wollin, G., D. B. Ericson, W. B. F. Ryan, and J. H. Foster (1971a), Magnetism of the Earth and climatic changes, *Earth Planet. Sci. Lett.*, *12*, 175–183.
- Wollin, G., D. B. Ericson, and W. B. F. Ryan (1971b), Variations in magnetic intensity and climatic changes, *Nature*, *232*, 549–551.
- Yue, X., L. Liu, W. Wan, Y. Wei, and Z. Ren (2008), Modeling the effects of secular variation of geomagnetic field orientation on the ionospheric long term trend over the past century, *J. Geophys. Res.*, *113*, A10301, doi:10.1029/2007JA012995.